



## Effect of the Target Size in the Calculation of the Energy Deposited Using PENELOPE Code

B. Leal-Acevedo<sup>1,2\*</sup>, P.G. Reyes-Romero<sup>2</sup>, F. Castillo<sup>3</sup> and I. Gamboadebuen<sup>1</sup>

<sup>1</sup>Institute of Nuclear Sciences, National Autonomous University of Mexico (UNAM), PO Box 70-543, 04510 Mexico City, Mexico

<sup>2</sup>Science Facultad, Autonomous University of the State Mexico, 100 Instituto Literario avenue, 50000 Toluca. Mexico

<sup>3</sup>Spectroscopy Laboratory, Institute of Physical Sciences, National Autonomous University of Mexico (UNAM), PO Box 48-3, 62251 Cuernavaca Morelos, Mexico

\*Email: benjamin.leal@nucleares.unam.mx

### ARTICLE INFORMATION

Received: June 14, 2018

Revised: July 07, 2018

Accepted: July 15, 2018

Published online: August 6, 2018

#### Keywords:

Specific energy; Linear energy, PENELOPE code

DOI: [10.15415/jnp.2018.61011](https://doi.org/10.15415/jnp.2018.61011)

### ABSTRACT

The specific and linear energy was calculated in target sizes of 10  $\mu\text{m}$ , 5  $\mu\text{m}$ , 1  $\mu\text{m}$ , 60 nm, 40 nm and 20 nm by taking into account the contribution of the primary photon beams and the electrons generated by them in LiF: Mg, Ti (TLD-100). The simulations were carried out by the code PENELOPE 2011. Using different histories of primary particles, for each energy beams the mean deposited energy is the same, but to achieve a statistical deviation lower than 1% the value of  $10^8$  was fixed. We find that setting the values  $C1 = 0.1$   $C2 = 0.1$  and  $W_{ec} = W_{cr} = 50$  eV the time of simulation decreases around the 25%. The uncertainties (1 SD) in the specific energy increases with energy for all target sizes and decreases with target size, with values from 1.7 to 94% for 20 nm and between 0.1 and 0.8% for 10  $\mu\text{m}$ . As expected, the specific and linear energies decrease with target size but not in a geometrical behavior.

## 1. Introduction

In the 70s Kellerer and Rossi [1, 2, 3] laid the groundwork for the ICRU to include as base quantities, the specific energy ( $z$ ) and linear energy ( $y$ ) to be used in microscopic structures size, these quantities correspond to dose and LET in the macroscopic world. The importance of these magnitudes is useful in the fields where the size of the structures requires the determination of the energy deposited in nanometer volumes. For the physical systems some authors [4, 5] calculated the specific energy and lineal energy where the objective is to obtain the frequency distribution for several sources and spherical water targets. In the last two decades it has been studied with special interest the capabilities of several programs using the Monte Carlo code, evaluating the position of a single interaction and the energy deposited by the secondary electrons with a lower energy threshold, regardless of the primary particle beam targets with micrometer or smaller sizes. This has been done by using simulations called event-by-event, where the coordinates of energy transfer and the energy deposited in the event are obtained [6, 7, 8]. Olko *et al.* [9] used electron transport in water vapor of unit density to determine the mean linear energy and the relative TL efficiency for LiF:Mg,Cu,P with a target sized of 60 nm and for  $\text{Al}_2\text{O}_3\text{:C}$  with target

sized of 170 nm. The aim of this work is to investigate the interaction of monoenergetic low energy photons in the TLD-100 chip using the PENELOPE code, considering the geometry used in experiments performed to determine the relative TL response and efficiency of TLD-100 for photons beams, for different sizes of the target volume.

## 2. Materials and Methods

In this work we used PENELOPE (version 2011) [10] where is necessary an input file that holds the geometrical information of the problem, the material and the energy and position of the source. In order to keep simple the simulation we fix the geometry of the TLD chip, the beam (point parallel beam using  $\alpha = 0$ ) and the TLD material (LiF:Mg,Ti). To calculate the specific energy ( $z$ ) and linear energy ( $y$ ) photon energies from 10 to 1250 keV as the primary beam were used. To achieve CPE, around the TLD was placed a layer of PMMA with thickness according to X-ray beam energy. During this work was analyzed the behavior of the statistical uncertainty in the absorbed energy due to different primary histories, from  $10^6$  to  $10^8$  primary particles. The average and maximum specific energy ( $z$ ) were obtained in target sizes of 10  $\mu\text{m}$ , 5  $\mu\text{m}$ , 1  $\mu\text{m}$ , 60 nm, 40 nm and 20 nm.

To determine the values of the elastic scattering dimensionless parameters C1 and C2, the cutoff energy for inelastic collisions for electrons  $W_{cc}$  and the bremsstrahlung cutoff energy  $W_{cr}$ , that will be use in the simulation, three combinations of values were compared to allow us to obtain the dose and kerma in LiF. For dose, the primary photons generated secondary electrons, which were followed by the code, while for the kerma, photons deposited on the first interaction all their energy. The deposited energy as a function of depth from the source position to the last layer of PMMA was obtained, which allowed us to analyze the behavior of the beam in the different layers of materials. For all the beams the cut-off energies were set up to 100 eV for the case of photons and positrons and 50 eV for electrons,  $C1 = C2 = 0.1$  and the values for  $W_{cc} = W_{cr} = 50$  eV. The beam was at the center of the TLD impinging on an arrange of  $1 \times 1 \times 300$  cubes (a raw of 300 cubes in the beam axis) for 20 nm to  $1 \mu\text{m}$ ,  $1 \times 1 \times 180$  for the case of  $5 \mu\text{m}$  and  $1 \times 1 \times 90$  for  $10 \mu\text{m}$ . From the calculation was obtained the specific energy for each volume size and then, dividing the energy imparted by the length cord, was calculated the linear energy.

### 3. Results

Using different histories of primary particles, for each energy beam the mean deposited energy is the same, but to achieve a statistical deviation lower than 1% the value of  $10^8$  was fixed. The statistical difference increases as function of the energy beam. The values of C1, C2,  $W_{cc}$  and  $W_{cr}$  analyzed include the recommendation of the manual that implies that C1 and C2 have value of 0.1 and  $W_{cc}$  and  $W_{cr}$  needs to be an energy two orders lower than the energy of the primary beam. In table 1 it is shown the combinations of values for these parameters for the case of cubes of 60 nm and a 1250 keV beam. From figure 1 it can be seen that the variation of those parameters from table 1 do not modify the absorbed dose in the volume of interest but the time of simulation decreases around the 25% for the case of  $C1 = C2 = 0.1$  and  $W_{cc} = W_{cr} = 50$  eV.

**Table 1.** Values of the mean free path between hard elastic events, maximum average fractional energy loss, cutoff energy for inelastic collisions for electrons and bremsstrahlung cutoff energy used to optimized the simulation time.

C1	C2	$W_{cc}$ (eV)	$W_{cr}$ (eV)	Nomenclature
0.1	0.1	12500	12500	a
0.1	0.10	50	50	b
0.2	0.2	0	0	c
0	0	0	0	d

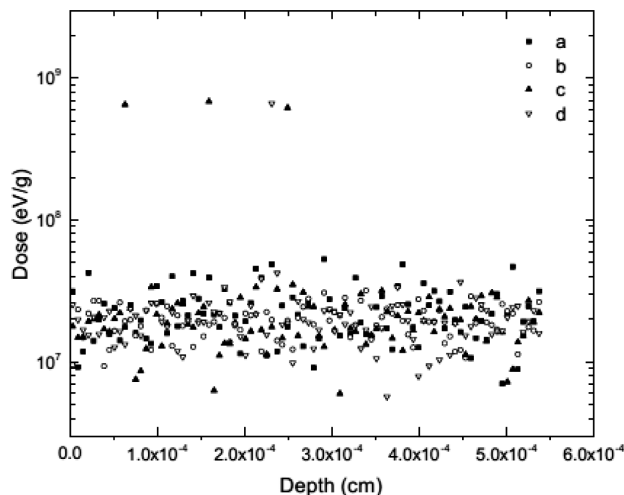


**Figure 1.** Dose as a function of depth for cubes of 60 nm and a 1250 keV beam for the combination of the parameters values shown in Table 1.

The average and the maximum specific energies as a function of beam energy are shown in figure 2, where for all target sizes, the maximum specific energy decreases, has a minimum value at about 70 keV and then increases with energy and decreases with the size of the target. This behavior takes place because, although the probability of interaction decreases with the beam energy, the range of secondary electrons increases with energy, so it is more probably that electrons released by higher energy beams in a given volume deposit their energy into another, increasing the maximum specific energy. The same behavior is observed for the average specific energy, except for target sizes greater than 1 mm and at low energies where  $Z_{avg}$  is lower for 10 keV than for 15 keV due to beam attenuation. The uncertainties (1 SD) in the specific energy increases with energy for all target sizes and decreases with target size, with values from 1.7 to 94% for 20 nm and between 0.1 and 0.8% for 10 mm.

As can be seen in figure 3, the maximum specific energy decreases rapidly, with target size (TS). The geometrical behavior is proportional  $1/TS^3$ , meanwhile the  $Z_{max}$  goes about  $1/TS^2.4$ , this might be because the probability of secondary electrons scattered away from the incident direction without depositing energy in the smallest targets. In this work we calculate the specific energy by taking into account the contribution of the primary beam and at the same time the contribution of secondary electrons, as a comparison we get the same behavior ( $Z$  decreases with TS with a power lower than 3) than that obtained by Olko [11] for the case of photons of Cs-137 striking spherical water targets.

In figure 4 it is shown the lineal energy decreases a function of the target size as seen in calculations in spherical water targets [11]. The difference between the geometric behavior (inversely proportional to  $2L/3$ ) can also be due to the effect of the secondary electrons that leave the target.

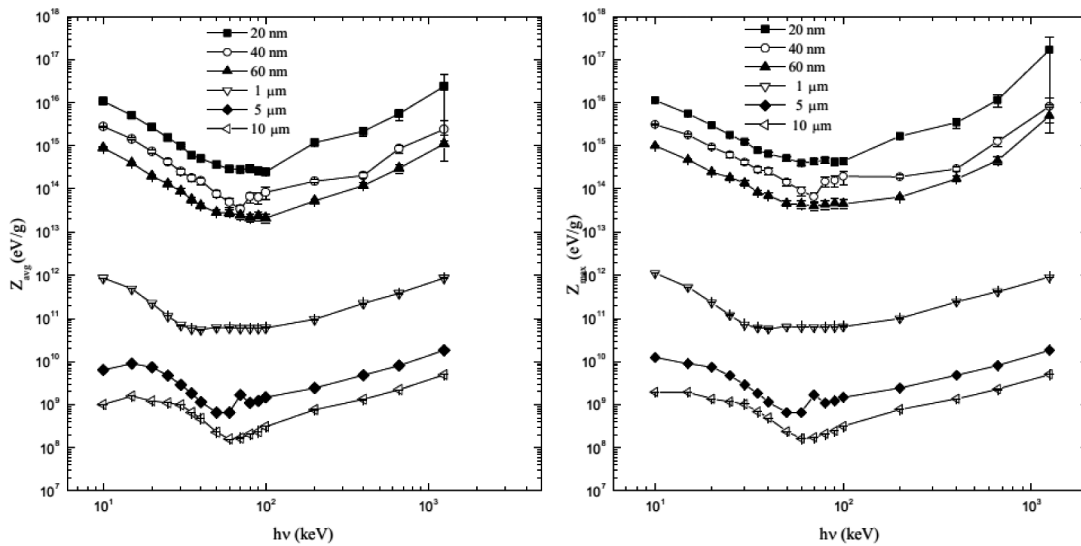


Figure 2. Average and maximum specific energies as a function of photon beam energy calculated for target sizes from 20 nm to 10 mm.

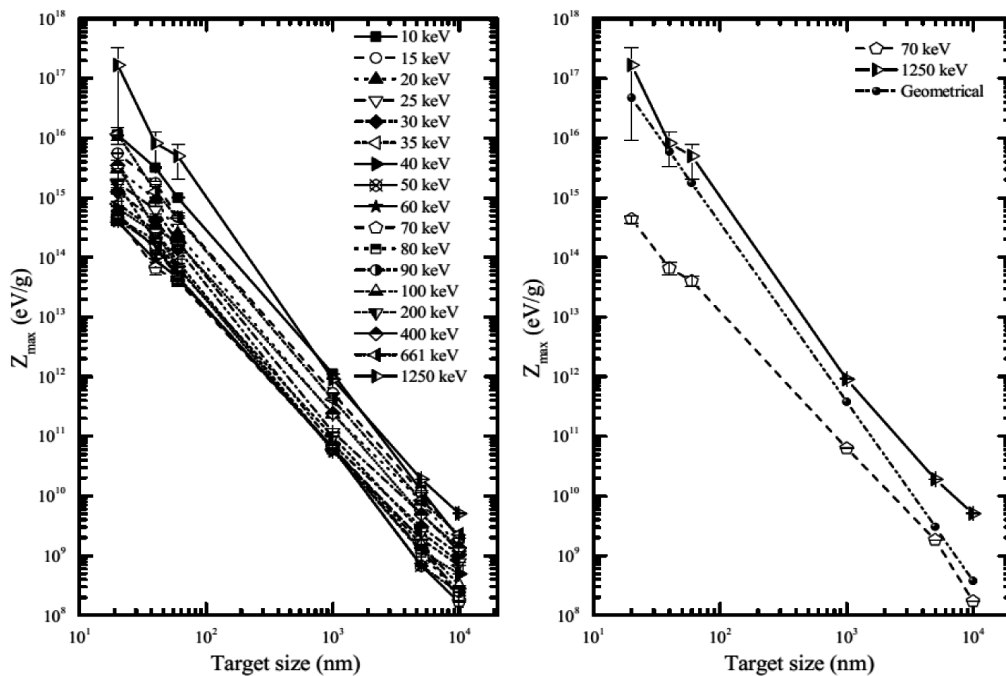
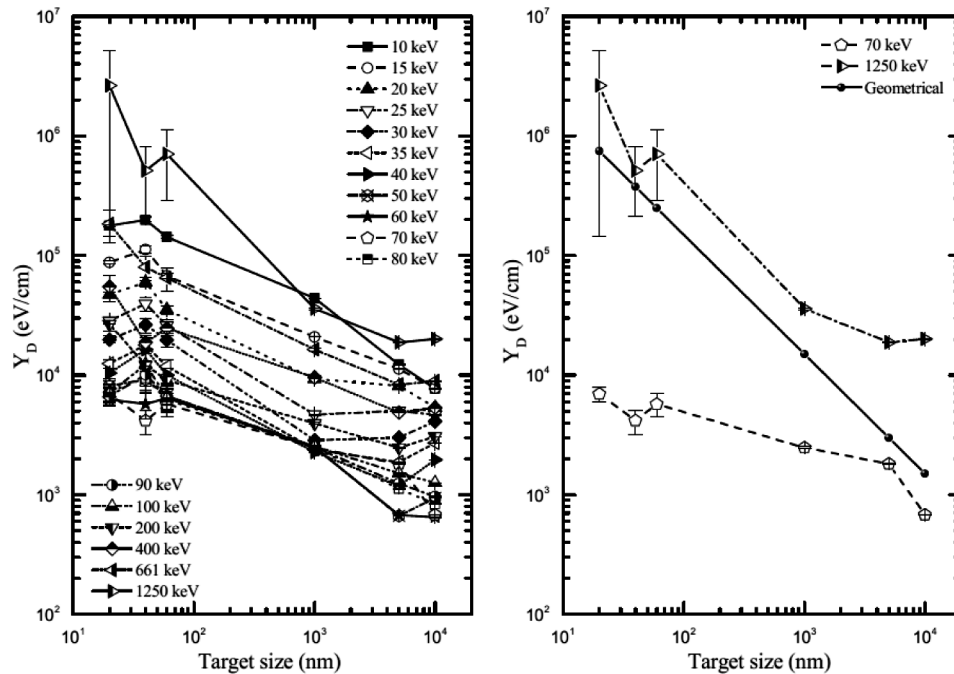


Figure 3. Maximum specific energy as a function of target size for all energies (Left) and for the energies with the lower and greater values of  $Z_{max}$  and the geometrical behavior (Right).

#### 4. Conclusions

The specific and linear energies, obtained for both the primary photons and secondary electrons at the same time, are in good agreement with those reported for spherical water targets [11]. As expected, the specific and linear energies decrease with target size but not in a geometrical

behavior. This can be due to the effect of the secondary electrons that leave the target without depositing energy in the smallest targets. It is recommended to analyze by means of the space-phase file the contribution of second generation particles to understand the way of how energy is deposited in micrometric volumes.



**Figure 4.** Lineal energy as a function of target size for all energies (Left) and for the energies with the lower and greater values of YD and the geometrical behavior (Right).

## Acknowledgment

The authors want to thank the support on computational work done by Antonio Ramírez Fernández, Juan Luciano Díaz González, Juan Eduardo Murrieta León, Enrique Palacios Boneta and Martín Cruz Villafañe

## References

- [1] M. Bernal and J. Liendo, *Med Phys* **36**, 620–625, (2009). <https://doi.org/10.1118/1.3056457>
- [2] A. Kellerer and D. Chmelevsky, Concepts of microdosimetry, I. Quantities. *Radiat Environ Biophys* **12**, 61–69, (1975). <https://doi.org/10.1007/BF02339810>
- [3] A. Kellerer and D. Chmelevsky, *Radiat Environ Biophys* **12**, 205–216 (1975). <https://doi.org/10.1007/BF01327348>
- [4] P. Olko, *Radiat Prot Dosimetry* **65**, 151–158, (1996). <https://doi.org/10.1093/oxfordjournals.rpd.a031610>
- [5] P. Olko, *Henryk Niewodniczanski Institute of Nuclear Physics*. (2002).
- [6] P. Olko, P. Bilski, M. Budzanowski, L. Czopyk, J. Swakon, *et al.*, *Radiat Prot Dosimetry* **122**, 378–381, (2006). <https://doi.org/10.1093/rpd/ncl46>
- [7] H. Rossi, *Radiat Environ Biophys* **17**, 29–40, (1979). <https://doi.org/10.1007/BF01323118>
- [8] F. Salvat, J. M. Fernández-Varea and J. Sempau, PENELOPE-2011: A Code System for Monte Carlo Simulation of Electron and Photon Transport (No. NEA/NSC/DOC (2011) 5). In *Nuclear Energy Agency. Workshop Proceedings. Barcelona*, (2011).
- [9] B. Scott and H. Schöllnberger, *Radiat Prot Dosimetry* **91**, 377–384, (2000). <https://doi.org/10.1093/oxfordjournals.rpd.a033247>
- [10] F. Villegas, N. Tilly and A. Ahnesjö, *Phys Med Biol* **58**, 6149–6162, (2013).
- [11] F. Villegas, N. Tilly, G. Bäckström, A. Ahnesjö, *Phys Med Biol* **59**, 5531–5543, (2014). <https://doi.org/10.1088/0031-9155/59/18/5531>